Appl Water Sci (2011) 1:19–24
DOI 10.1007/s13201-011-0004-3

ORIGINAL ARTICLE

# Photodegradation of bromophenol blue with fluorinated $TiO_2$ composite

**L. N. Dlamini · R. W. Krause · G. U. Kulkarni · S. H. Durbach**

Received: 30 March 2011 / Accepted: 5 May 2011 / Published online: 7 June 2011


**Abstract** Fluorinated $TiO_2$ composites were prepared by the sol–gel method. The photocatalytic activities of the composites were evaluated with bromophenol blue (BPB). Composites which contained carbon nanotubes showed the highest photodegradation (98%) of BPB at 20 min as compared to pure $TiO_2$. Photodegradation by-products of BPB such as $Br^-$ and $[SO_4]^{2-}$ ions were monitored with ion chromatography. All catalysts were characterized with microscopic techniques, including transmission electron microscopy and scanning electron microscopy which were both equipped with an energy dispersive X-ray spectrophotometer. The polymorph of $TiO_2$ was verified by the use of Raman spectroscopy and powder X-ray diffraction.

**Keywords** Bromophenol blue · Fluorinated $TiO_2$ · Photodegradation · Carbon nanotubes

L. N. Dlamini (✉) · R. W. Krause
Department of Chemical Technology, UJ Centre for Nanomaterials Science, University of Johannesburg, Box 17011, Doornfontein 2028, South Africa
e-mail: lndlamini@uj.ac.za

G. U. Kulkarni
Chemistry and Physics of Materials Unit, Jawaharlal Nehru Centre for Advanced Scientific Research, Jakkur, Bangalore 560064, India

S. H. Durbach
Molecular Sciences Institute, School of Chemistry, University of the Witwatersrand, Johannesburg 2050, South Africa

L. N. Dlamini · R. W. Krause · S. H. Durbach
Centre of Excellence in Strong Materials, School of Chemistry, University of the Witwatersrand, Johannesburg, South Africa

## Introduction

Wastewaters containing organic pollutants, such as dyes from textile industries are of concern because of their hazardous effects on the environment (Smith et al. 2009). Their presence in water, even at low concentrations has been the driving force for improved water treatment techniques. An example of such dyes is bromophenol blue (BPB), the structure of which is shown in Fig. 1 (Masere and Pojman 1998). This compound has absorption characteristics for $\lambda_{max}$ of 589 and 435 nm at pH 4.6 and 3.0, respectively.

Titanium dioxide ($TiO_2$) is the preferred photo-catalyst for water treatment, because of its low cost, high stability, and non-toxicity particularly for the mineralization of organic pollutants (Lensebigler et al. 1995; Fujishima and Honda 1972). However, the use of $TiO_2$ is hampered by two primary factors. The first is the fast recombination rate of photo-generated electron/hole ($e^-/h^+$) pairs. The second is the large band gap (3.2 eV) which makes $TiO_2$ incapable of utilizing visible light, that accounts for about 50% of solar energy (Lensebigler et al. 1995; Fujishima and Honda 1972; Ni et al. 2009).

Therefore, to improve the performance of $TiO_2$ and enhance its photo-catalytic activity, several modifications have been suggested: such as noble metal loading, anion doping and dye sensitisation (Lensebigler et al. 1995; Ni et al. 2009). The use of metals as dopants has several drawbacks, including reduced thermal stability as well as the fact that metal centres act as recombination centres which allows for fast recombination of the produced electron/hole pairs (Lensebigler et al. 1995; Ni et al., 2009). All the mentioned drawbacks result in decreased photo-catalytic efficiency. The toxicity and instability of dye-sensitized $TiO_2$ limits its application in photo-catalysis.

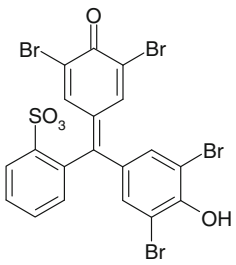


**Fig. 1** Structure of bromophenol blue

However, anion-doped $TiO_2$ [N, (Ashi et al. 2001, Kontos et al. 2011); F, (Minero et al. 2000a; Selli et al. 2011; Chen et al. 2009); S, (Ohno et al., 2004); C, (Sakthivel and Kisch 2003; Matos et al. 2010)] have shown reduced effective band gaps and improved photocatalytic activity.

Mrowetz and Selli (2005) have experimentally demonstrated that fluorination of $TiO_2$, enhanced photocatalytic activity by generating hydroxyl radicals. The increased of free hydroxyl radicals results in an increase in the rate of degradation of organic pollutants. Also, the recombination of holes and electrons is minimized with fluorination, thus further enhancing photo-catalytic activity of $TiO_2$.

Composites containing CNTs have the potential to be used in various applications as they exhibit synergistic effects between the metal oxide and carbon phase (Eder and Windle 2008). CNTs/$TiO_2$ composite materials have also been shown to increase the rate of photocatalytic oxidation of organic pollutants. In this paper, we present the synthesis and characterization of a composite of fluoride-doped $TiO_2$ with CNTs and the evaluation of its photoactivity with BPB.

## Experimental

### Catalyst preparation

One step fluorination of $TiO_2$ with CNTs was successfully achieved via a sol–gel process. Commercial multi-walled CNTs (400 mg) with a diameter range of 110–170 nm and 5–9 μm length were refluxed in nitric acid (50 mL) for 16 h. This was done to introduce functional groups on the surface of CNTs. The functionalized CNTs (0.2% m/m) were sonicated in 10 mL *n*-butanol for 15 min. The dispersed CNTs were mixed with titanium butoxide (10 mL) and *n*-butanol (42 mL). The mixture was stirred continuously for 30 min and followed by the addition of formic acid (11 mL) (Zhu et al. 2005). Once a grey precipitate was formed.

$NH_4F$ (10 mL, 20% m/m) prepared in 20 mM HF was added. The pH was maintained at 2, to allow for the exchange of hydroxyl ion with fluoride ions. The precipitate was stirred for 2 h and aged for another 2 h. After the precipitate had been washed with *n*-butanol and water, it was dried for 2 h at 80°C to remove most of the solvent. The dried sample was ground to fine powder and calcined in the furnace at a ramp rate of 10°C/min to a maximum temperature of 400°C in air for 4 h. Pure $TiO_2$ and CNTs-$TiO_2$ were also prepared, following the same method.

### Characterization

X-ray scattering patterns were scanned by analyzing the powdered samples using a Siemens Seifert 3000TT diffractometer using Cu Kα (0.1540 nm) monochromatic beam. The power settings of the source were 40 kV and 40 mA. Diffraction patterns were taken with a scan rate of 5°/min over the range $20° \leq 2\theta \leq 60°$. The average crystal sizes, $d$, of anatase were determined by the Scherrer equation for a given phase $\theta$, at an X-ray wavelength $\lambda$ 0.1540 nm and FWHM (full width at half maximum, $\beta$).

$$d = \frac{0.89\lambda}{\beta \cos\theta} \quad (1)$$

Scanning electron microscopy (SEM) images were taken at an accelerated voltage of 2 kV using a Nova NanoSEM 600 instrument (FEI Co., The Netherlands) equipped with an X-ray detector for energy dispersive X-ray analysis (EDX) operated at 15 kV. Transmission electron microscopy (TEM) images were captured using JEOL-3010 microscope at an accelerated voltage of 200 kV. Samples were dispersed in methanol and drop-dried on a copper grid. Raman spectra were collected with a Horiba Jobin–Yvon spectrometer at an ambient temperature using an ($Ar^+$) excitation source of 514.5 nm, with a spectral resolution of 2 $cm^{-1}$. The laser power at the sample was about 3.0 mW. The laser beam was focused onto the sample by a 100× magnification objective lens of an Olympus microscope.

### Photocatalytic measurements

Bromophenol blue was used as a model pollutant to evaluate the photocatalytic activity of the prepared catalysts. Each of the four ($TiO_2$, CNTs-$TiO_2$, $TiO_2$-F and CNTs-$TiO_2$-F) catalysts (0.1 g) was suspended in a solution of BPB (100 mL, 10 $mgL^{-1}$). Prior to the irradiation, the reaction vessel was magnetically stirred for 30 min to ensure an adsorption/desorption equilibrium in the dark. The photodegradation was initiated by a UV lamp (55 Watts) at 366 nm and the cabin temperature was measured to be at 45 ± 5°C for all devices. Sample aliquots (5 mL) were taken at regular intervals (20 min) and filtered through 0.45 μm Teflon membranes.

The degradation of BPB was monitored by measuring the absorbance at $\lambda = 435$ nm as a function of irradiation

time with a UV–vis spectrophotometer (Shimadzu UV-2450). The resulting $Br^-$ and $[SO_4]^{2-}$ ions were measured with an ion chromatograph (IC, Dionex-ICS 2000) that was equipped with a Dionex Ion Pac AS18 (2 × 250 mm) column and a conductivity. The eluent solution was 30 mM KOH. In this study, the photocatalytic degradation was calculated as the following formulae:

$$\text{Amount degraded} = (C/C_0) \quad (2)$$

where $C_0$ and $C$ are the initial and final concentrations of BPB at $t = 0$ and $t$.

## Results and discussion

Figure 2 shows the XRD patterns of $TiO_2$ and CNTs-$TiO_2$, containing 0.2% m/m of CNTs. Intense peaks at $2\theta = 25.5$, 38.2, 48.6, 54.0 and 55.3°, corresponding to crystal planes of $TiO_2$ anatase (101), (004), (200), 108) and (211), respectively, using JCPDS card 04047 (Diebold 2002). All of the patterns and planes can be exclusively assigned to anatase, a polymorph of $TiO_2$, which is reported to be photocatalytically superior to the other forms of $TiO_2$ (Smith et al. 2009). By applying the Scherrer equation for (101) reflection, the average size of $TiO_2$ was calculated to be 20 nm. The Raman spectra shown in Fig. 3 also assign the 144 $cm^{-1}$ (very strong $E_g$), 397 $cm^{-1}$ ($B_{1g}$), 516 $cm^{-1}$ ($A_{1g}$) and 639 $cm^{-1}$ ($E_g$) bands to anatase as confirmed by XRD. Raman analysis of the CNTs-$TiO_2$ composite indicates the presence of the G band at 1,611 $cm^{-1}$ resulting from CNTs, indicating the crystalline nature of CNTs.

TEM and SEM images in Fig. 4 reveal that the $TiO_2$ particles were partly agglomerated and yet their average size distribution was uniform. Both microscopic techniques

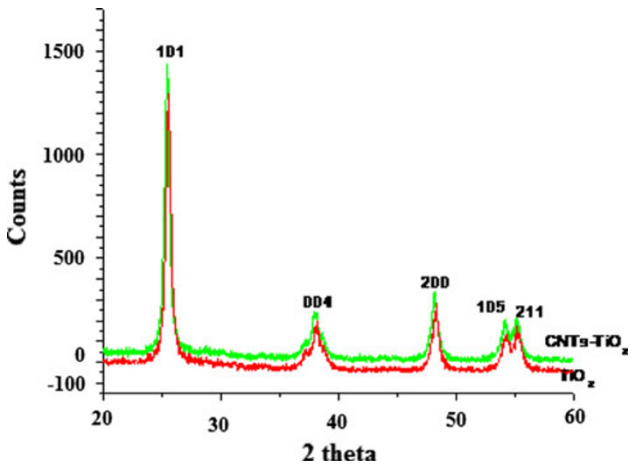


**Fig. 2** XRD pattern of $TiO_2$ and CNTs-$TiO_2$

estimated the average particle size to be 16 nm, similar to XRD estimates. An elemental composition of the composite was elucidated with EDX and confirmed the presence of carbon, fluorine, titanium and oxygen.

Rapid photocatalytic degradation of BPB by CNTs-$TiO_2$-F was observed with a percentage removal of 98% of BPB at 20 min of illumination. Complete mineralization of BPB was maintained throughout the irradiation time. The as-prepared $TiO_2$ showed the least photoactivity of all four catalysts, managing to degrade up to 85% of BPB at 140 min. CNTs-$TiO_2$ and $TiO_2$-F, degraded BPB up to 94% in140 min irradiation time. The reaction kinetics all show that the reactions followed a pseudo first order, increasing from 0.0178 $min^{-1}$ ($TiO_2$) to 0.0673 $min^{-1}$ (CNTs-$TiO_2$-F) (Fig. 5).

The degradation efficiency of the CNTs-$TiO_2$-F was the highest, because CNTs are excellent electron transporters. Delocalization of $\pi$-bonds that form from unhybridized p-orbitals (Eder 2010), allows CNTs to be conducting; thus efficiently separating electrons from holes, as in Scheme 1 (Eder 2008). This can be attributed to the high percentage degradation of BPB due to the high surface area of CNTs that also enhances the adsorption of BPB to be degraded by $TiO_2$.

Fluorinated $TiO_2$ catalyst degraded BPB efficiently because of the excess production of free radicals as compared to pure $TiO_2$. When $TiO_2$ is fluorinated, the surface ($\equiv$ Ti $\rightarrow$ F) acts as an electron-trapping site, tightly holding the electrons (due to the high electronegativity of fluorine), thereby minimizing chances of recombination (Minero et al. 2000a, b; Mrowetz and Selli 2005). This then leads to increased photocatalytic activity, of $TiO_2$-F with BPB. Furthermore, since fluoride ions have a high potential (3.6 V), valence band holes do not directly oxidize the surface of titanium, but directly react with water molecules, producing more OH· radicals as illustrated by (3) (Mrowetz and Selli 2005; Park and Choi 2004). An increase in hydroxyl radical production enhances the photocatalytic degradation of BPB. Preliminary experiments conducted in our laboratories with 2,2–diphenyl-1-picryhydrazyl (DPPH) also showed that more hydroxyl radicals were liberated with fluorinated $TiO_2$ as compared to un-fluorinated catalyst.

$$\equiv \text{Ti} - \text{F} + \text{h}^+_{\text{VB}} + \text{H}_2\text{O} \rightarrow \text{OH}\cdot_{(\text{free})} + \text{H}^+ + \equiv \text{Ti} - \text{F} \quad (3)$$

To verify the degradation of BPB the liberation of $Br^-$ and $[SO_4]^{2-}$ ions were measured with an IC. As illustrated, in Fig. 6, $Br^-$ ions were liberated at much higher amounts than the $[SO_4]^{2-}$ ions for all four catalysts, confirming that all four bromine atoms were removed from BPB in the case of fluorinated $TiO_2$.

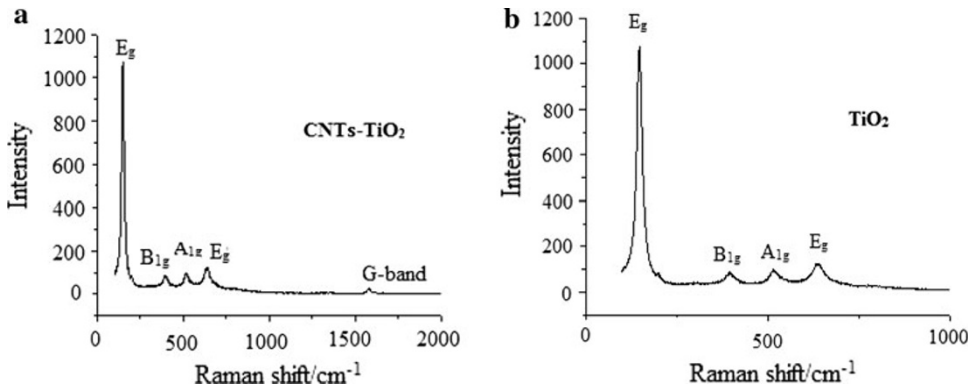


**Fig. 3** Raman spectra of **a** CNTs-$TiO_2$ and **b** $TiO_2$

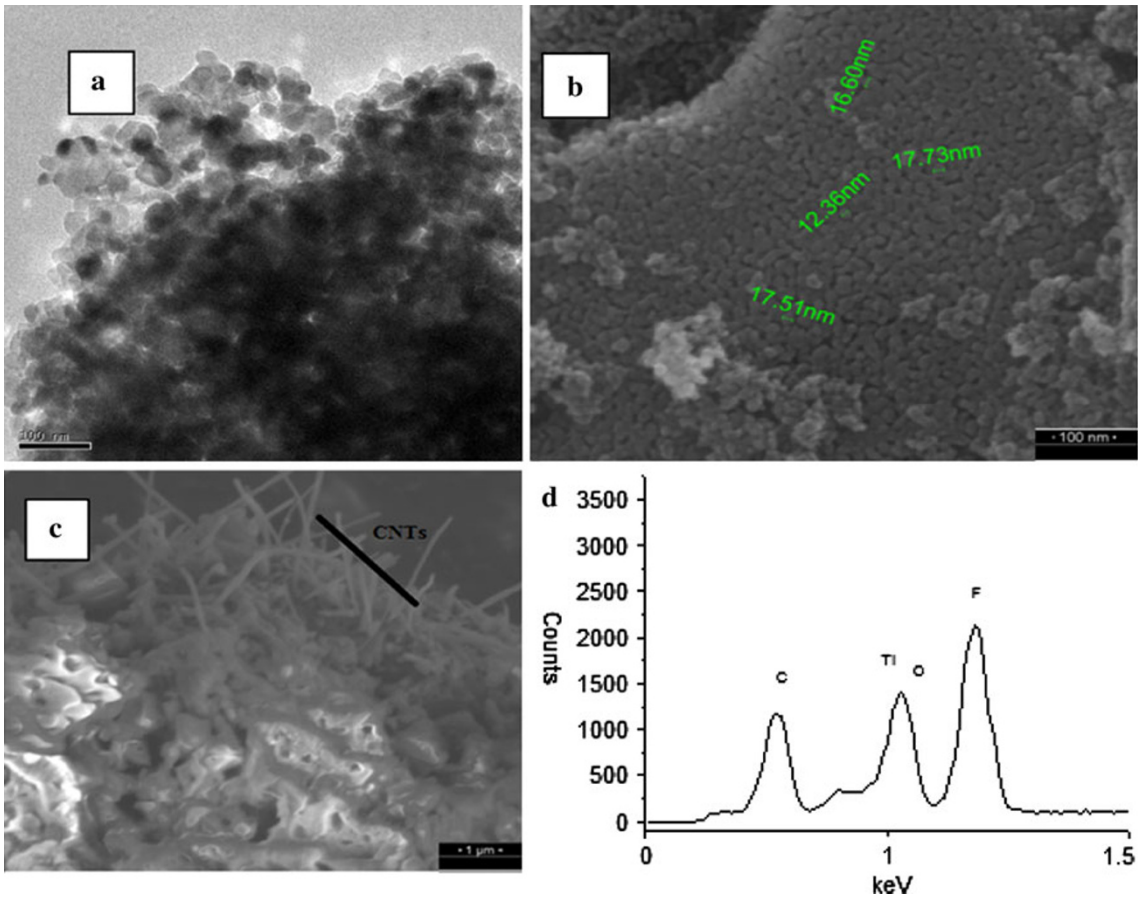


**Fig. 4** **a** TEM and **b** SEM images of $TiO_2$ and **c** CNTs-$TiO_2$, and **d** EDX spectrum of CNTs-$TiO_2$-F

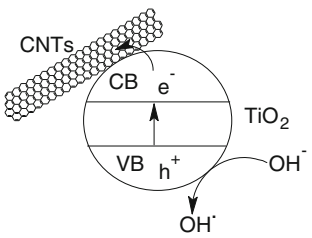


**Scheme 1** CNTs acting as electron carries in CNTs-$TiO_2$ hybrid

The degradation mechanism of organic dyes from the use of $TiO_2$ proceeds via the formation of $e^-/h^+$ pairs upon illumination with energy greater or equal to 3.2 eV (4). The generated holes may then react with water producing OH· radicals (5). These OH· radicals are powerful oxidizing agents which can then degrade the organic dye (6). However, the degradation of the dye can also be achieved via the direct reaction of the generated holes (7). In addition to the mentioned possible degradation pathways involving

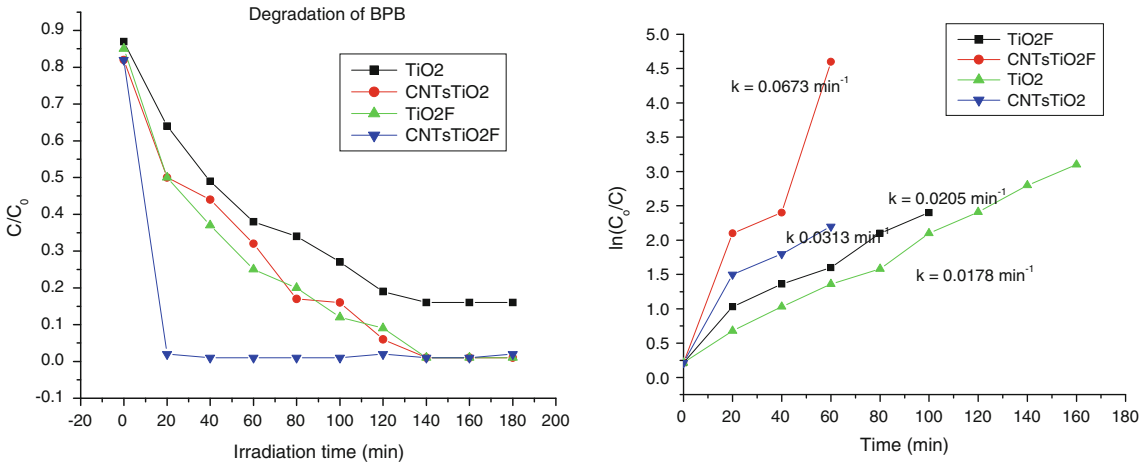


**Fig. 5** Degradation of BPB by the four catalysts and reaction kinetics

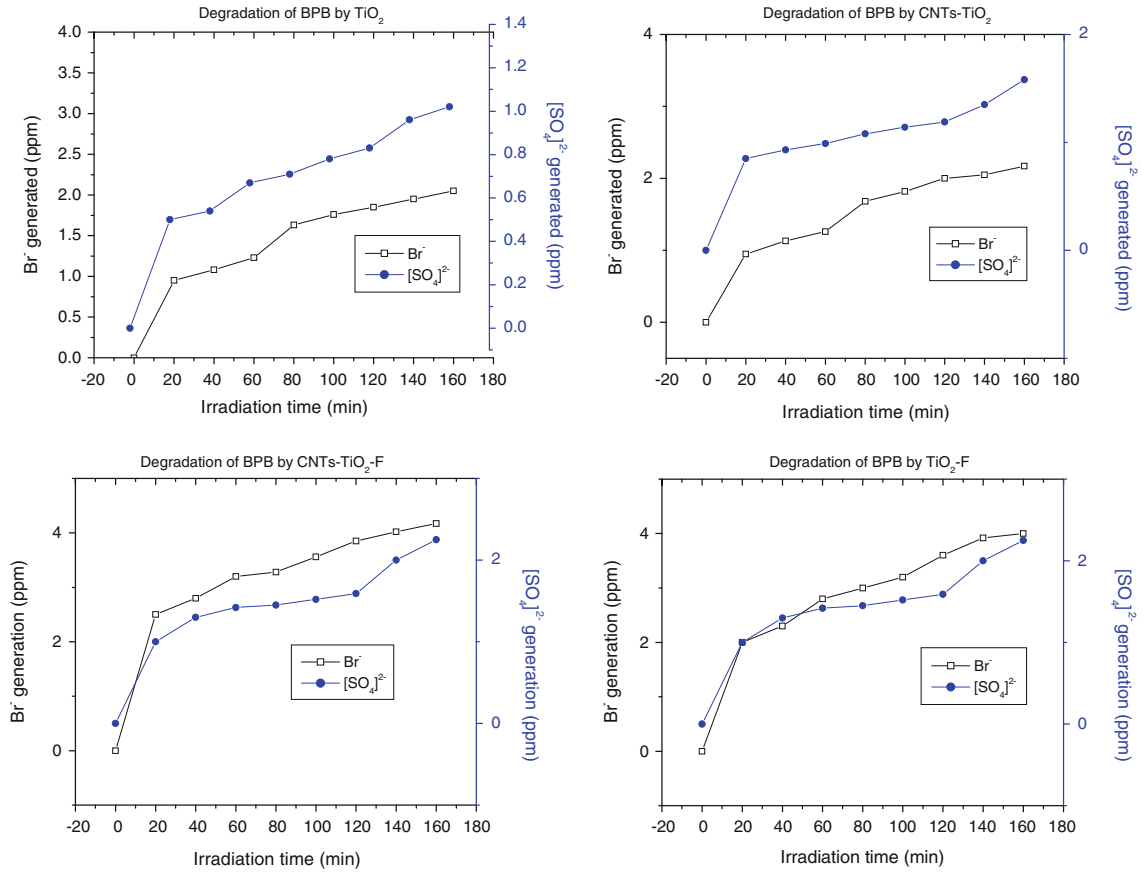


**Fig. 6** Liberated $Br^-$ and $[SO_4]^{2-}$ ions measured by IC, for the four catalysts

holes, the photogenerated electrons can either reduce the dye or can act with the electron acceptor to create a superoxide, $O_2^-$ thereby mineralizing the dye (8). (Lensebigler et al. 1995; Ni et al. 2009; Kudo and Miseki 2009):

$$TiO_2 + h\nu \rightarrow TiO_2\left(e_{CB}^- + h_{VB}^+\right) \quad (4)$$

$$TiO_2\left(h_{VB}^+\right) + H_2O \rightarrow TiO_2 + H^+ + OH\cdot \quad (5)$$

$$Dye + OH\cdot \rightarrow Degradation\ products \quad (6)$$

$$Dye + h_{VB}^+ \rightarrow Oxidation\ products \quad (7)$$

$$TiO_2\left(e_{CB}^-\right) + O_2 \rightarrow TiO_2 + O_2^- \quad (8)$$

## Conclusion

$TiO_2$ nanocomposites were successfully synthesised and characterized with microscopic (TEM and SEM) and spectroscopic (XRD and Raman) techniques. CNTs-$TiO_2$-F had the highest photocatalytic activity of BPB, 98% removal in 20 min irradiation time, while prepared $TiO_2$ showed the least activity of 85% in 120 min. The high photocatalytic activity of CNTs-$TiO_2$-F can be attributed to the increase in production of OH· radicals as attested by previous studies. The efficiency of the composite is also enhanced by efficiently maximizing the separation of electrons from holes by CNTs, as they act as electron transporters. The liberation of Br- and $[SO_4]^{2-}$ ions confirms the mineralization of the dye. Kinetics measurements revealed that the photodegradation followed a pseudo first order kinetics.

**Acknowledgments** Funding from the University of Johannesburg, ESKOM's Tertiary Support Program (TESP) and the Department of Science and Technology, Centre of Excellence in Strong Materials (DST/CoESM) is appreciated. LN Dlamini thanks Dr. Sharon Moeno for her assistance.



## References

Ashi R, Morikawa T, Ohwaki T, Aoki K, Taga Y (2001) Visible-light photocatalysis in nitrogen-doped titanium oxides. Science 293:269–271

Chen Y, Chen F, Zhang J (2009) Effect of surface fluorination on the photocatalytic and photoinduced hydrophilic properties of porous $TiO_2$ films. Appl Surf Sci 255:6290–6296

Diebold U (2002) The surface of titanium dioxide. Surf Sci Rep 48:53–229

Eder D (2010) Carbon nanotube—inorganic hybrids. Chem Rev 110:1348–1385

Eder D, Windle AH (2008) Carbon-inorganic hybrid materials: the carbon nanotube/$TiO_2$ interface. Adv Mater 20:1787–1793

Fujishima A, Honda K (1972) Electrochemical photolysis of water at a semiconductor electrode. Nature 72:108–114

Kontos AG, Pelaez M, Likodimos V, Vaenas N, Dionysiou DD, Falaras P (2011) Visible light induced wetting nanostructured N–F co-doped titania films. Photochem Photobiol Sci 10:350–354

Kudo A, Miseki Y (2009) Heterogeneous photocatalyst materials for water splitting. Chem Soc Rev 38:253–278

Lensebigler AL, Lu G, Yates JT (1995) Photocatalysis on $TiO_2$ surfaces: principles, mechanisms and selected results. Chem Rev 95:735–758

Masere J, Pojman JA (1998) Free radical-scavenging dyes as indicators of frontal polymerization dynamics. J Chem Soc Faraday Trans 94:919–922

Matos J, Lopez EG, Palmisanol L, Garcia A, Marci G (2010) Influence of activated varbon in $TiO_2$ and ZnO mediated photo-assisted degradation of 2-propanol in gas-solid regime. Appl Catal B: Environ 99:170–180

Minero C, Mariella G, Maurino V, Pelizzetti E (2000a) Photocatalytic transformation of organic compounds in the presence of inorganic anion1. Hydroxyl-mediated and direct electron transfer reactions of phenol on titanium fluoride system. Langmuir 16:2632–2641

Minero C, Mariella G, Maurino V, Vione D, Pelizzetti E (2000b) Photocatalytic transformation of organic compounds in the presence of inorganic anion2. Competitive reactions of phenol and alcohols on a titanium dioxide fluoride system. Langmuir 16:8964–8972

Mrowetz M, Selli E (2005) Enhanced photocatalytic formation of hydroxyl radicals on fluorinated $TiO_2$. Phys Chem Chem Phys 7:1100–1102

Ni M, Leung MKH, Leung DYC, Sumathy K (2009) A review and recent developments in photocatalytic water-splitting using $TiO_2$ for hydrogen production. Renew Sustain Energy Rev 11:401–425

Ohno T, Akiyoshi M, Umebayashi K, Asai T, Mitsui T, Matsumura M (2004) Preparation of S-doped $TiO_2$ photocatalyst and their photocatalytic activities under visible light. Appl catal A 265:115–121

Park H, Choi W (2004) Effects of TiO surface fluorination on photocatalytic reactions and photoelectrochemical behaviours. Phys Chem B 108:4086–4093

Sakthivel S, Kisch H (2003) Daylight photocatalysis by carbon-modified titanium dioxide. Angew Chem Int Ed 42:4908–4911

Selli E, Dozzi MV, Livraghi S, Giamello E (2011) Photocatalytic activity of S- and F- doped $TiO_2$ in formic acid mineralization. Photochem Photobiol Sci 10:343–349

Smith YR, Kar A, Subramanian VR (2009) Investigation of physicochemical parameters that influence photocatalytic degradation of methyl orange over $TiO_2$ nanotubes. Ind Eng Chem Res 48:10268–10276

Zhu J, Zhang J, Chen F, Iino K, Anpo M (2005) High activity $TiO_2$ photocatalyst prepared by a modified sol-gel method: Characterization and their photocatalytic activity for the degradation of XRG and X-GL. Catalysis 35:261–268